Methods to evaluate earth slip cohesion to build with light earth

Théo Vinceslas, Thibaut Lecompte, Erwan Hamard, A. Hellouin de Menibus, Hélène Lenormand, Thibaut Colinart

Methods to evaluate earth slip cohesion to build with light earth.

Théo Vinceslas[1*], Thibaut Lecompte[1], Erwan Hamard[2], A. Hellouin de Ménibus[3,4], Hélène Lenormand[5], Thibaut Colinart[1]

corresponding author

1. Univ. Bretagne-Sud, UMR CNRS 6027, IRDL, F-56100 Lorient, *theo.vinceslas@univ-ubs.fr
2. IFSTTAR, MAST, GPEM, F-44344 Bouguenais
3. Eco-Pertica, Hôtel Buissonnet, F-61340 Perche-en-Nocé
4. Association Nationale des Chanvriers en Circuits Courts, Mas de Valus 30580 Bouquet
5. UniLaSalle, EA7519 (UniLaSalle Université d'Artois) F-76134 Mont-Saint-Aignan

Highlights.

- Cohesive behaviors of 6 earth are studied through yield stress measurement.
- The study is based on samples representative of Brittany and Normandy earth natural variability.
- Existing or new rheological tests are compared to evaluate their accuracy and validity range.
- Results allow to control an earth slip yield stress knowing its water content.

Abstract.
Bio-based materials are subject to a growing interest since the nineties to reduce the environmental impacts of the building sector. Light earth is a low impact insulation material. Light earth building methods are based on the use of earth slip, a mix of clayed earth and water, and aggregates or fibers. The earth slip is characterized on site by mason by different means. This study aims to compare different rheological measurements methods in laboratory conditions, and then to define simple and robust tests adapted to any conditions. The study is based on six soil samples. Geotechnical characterizations show that these soils cover a wide range of natural variabilities. Their cohesive behaviors were investigated by measuring the yield stress with a rheometer, a spread test, a dipping test and a rough wall cone test, both developed for the study, and a Marsh cone test. Accuracy and the validity range of each test are presented alongside the needs for light earth applications.

Keywords: clay, rheological behavior, yield stress, light earth

I Introduction

Earthen construction has been used for centuries with various building materials and methods, mainly rammed earth, wattle and daub, cob, adobe, and plasters. Recently, it has attracted renewed interest, especially due to its low environmental impact [1]–[5]. For instance, light earth is a contemporary material based on wattle and daub, developed since the 1920s [6] in Germany and the 1990s in France, to obtain satisfactory thermal insulation with clay as a binder. It consists in a mix of a large volume fraction (between 50 and 80%) of light aggregates bound together with a small quantity of a liquid earth slip (i.e. earth and water). The aggregates mostly used currently are straw [6], [7] and hemp [8], [9].

Even if the variability of the components can be tackled on site by experimented mason, it makes more complex scientific studies. Bio-based aggregates might differ in terms of particle size distributions and chemical compositions depending on the species, crop practices, harvesting, and the primary transformation process [10]. In lime-hemp literature, hemp variability impacts on the material performances are under studies [10].

On another hand, soils vary in composition and clayey behavior, even over short distances [11]. For raw earth construction, assessment of the suitability of one material for a given building technic is a subject of scientific studies [12]–[16].

Nowadays, the earth slip is qualitatively characterized on site by mason by different means. It is of interest to supplement such analysis by a quantitative estimation of earth slip rheological behavior with simple and rapid tests.

In unsaturated soils or dense earth building materials, the cohesion is defined by attraction between particles. This attraction is in majority driven by capillarity and specific forces between clay platelets [17]. Thus, soil cohesion appears to be a key parameter since the intrinsic cohesion of earth particles and the water content drives the rheological behavior of the slips. High slip cohesion allows a high volume fraction of bio-based aggregates and leads to good insulation properties in the hardened state. Standard geotechnical tests as particle size distribution, Atterberg limits and Methylene Blue Value (MBV) or Cation Exchange Capacity (CEC) [18]–[21] allow us to roughly estimate the cohesive and physical behavior of soils. But further tests are needed to quantify the earth slip cohesion as a function of its water content. An earth slip is a mix of fine particles (clay and silt), coarse particles (sand), and water. Such a granular suspension behaves as a yield-stress material [22]–[25], with a yield that depends on the cohesive behavior of clay and silt, particle size distribution, and solid volume fraction[26].

Some studies [2], [27]–[31] evaluate the rheological behavior of earthen material that are composed of a high solid volume fraction (mortars, rammed earth). Rheology is also used for the development of 3D-printed earth [32] or earth concretes [33]. But no large comparative studies are found on the evolution of the rheological behavior of different earth according to their content.

Even fewer studies deal with the development of simple rheological characterization tests [34]–[37]. For example, Alhaik et al. [38] use the flow test to characterize the impact of adding starch to earth mortars. Here, the flow test is used to define the water content in order to aim a given workability. But none of the studied mortars have the same rheological parameters and no link is done between the flow test and the rheology of the suspensions.

The main purpose of the present study is to assess different methods to measure the rheological behavior of the earth slips, in order to identify if a simple and robust test is adapted to field conditions. In the present study, characterization made on suspensions are carried out with simple rheological tests specifically developed for this study or from the literature [29]–[31], [34], and with a laboratory rheometer equipped with a Vane geometry tool. Tests from different areas were considered in this study: the spreading test is a well-used spread test in cement grout characterizations; the Marsh cone

is used for quarry sludge [35], [39]; the viscosity cups are used in the oil and painting industries [40] ; the rough wall cone test is especially developed as an adaptation of the latter two tests; and finally, the dipping cylinder test is derived from the plate test [41] used also for cement grout setting analyses.

Firstly, studied earth materials are presented along with their characteristics. In the second part, the theoretical frame of each previously mentioned test is described in details. Then, results of earth slip characterization are presented according each studied method. Finally, results are discussed following the suitability of each test for yield stress measurement.

CEC	Cation Exchange Capacity	p_0	Perimeter of the cylinder
A_{CEC}	Clay activity calculated on CEC	h	Immersed height
H_0	Initial height of spreading flow container	h_0	Height of the sheet
R_{0max}	Initial maximum radius of spreading flow container	H_c	Height of the Rough wall cone, without extension
R_{0min}	initial minimum radius of spreading flow container	β	Slope angle
V	Volume of spreading flow container	R_{max}	Rough wall cone maximum radius
ρ	Density	R_{min}	Rough wall cone minimum radius
g	Gravity	A_{cone}	Slope area
τ_0	Yield stress	R_f	Maximum radius on Marsh funnel
τ'_0	Dimensionless yield stress	R	Minimum radius on Marsh funnel
S	Slump	L	Height of cylinder part in Marsh funnel
S'	Dimensionless slump	H_s	Height of remaining material
R	Final spread radius	H_f	Height of the conical part of the Marsh funnel
V_0	Initial sample volume	v	Ratio of vertical stability in rheometer tests with vane tool
a	Parameter in Pierre calculation	h_c	Vane tool height
b	Parameter in Pierre calculation	k	Number of particles
M	Mass	$\emptyset_{max}$	Maximum particles diameter in earth slip
A	Plate area	I	Inertia
W'	Apparent weight	Cyl	Cylinder
W'	Weight	Sp	Sand paper
M_0	Sample Initial mass	λ	Thickness of sheared material in the air-material interfacial zone
A_0	Initial sheet area	α	Fitting parameter
t	Thickness of the remaining slip	w	Water content
T	Tensile force at inside/outside interface	ρ_e	Earth particles density
		ρ_w	Water density
		m	Sample mass

Table 1 *Classification*

98

II Materials

2-1- Earth identification

Six soil samples were chosen among 27 samples collected in Brittany and Normandy (France) in order to investigate a large range of variabilities. One reference had been used by builders on more than 15 hemp-earth constructions, and the other five came from different locations, such as quarries, where it is possible to sample raw soils or washing sludge, or private lands, where the soil was used for construction, using the knowledge of experienced builders, which facilitated selecting soils with "extreme" characteristics. Apart from the reference (REF), the five other soil samples were given numbers. Each collected soil sample was examined using traditional geotechnical characterization methods. One goal was to evaluate if the selected samples cover a large variability range of soils that can be found in nature.

Specific densities were measured using a water pycnometer according to the French standard NF P94-054 [42]. According to this standard, the soil is prepared by wet sieving at 2 mm, which is the sieve usually used for earth slips. Particle size distribution was quantified by dry sieving for the coarse fraction (above 80 µm), according to NF P 94-056 and by a hydrometer test for the fine fraction (below 80 µm), according to NF P 94-057. The cation exchange capacity (CEC) was measured with cobalt hexamine according to NF ISO 23470. Atterberg limits were measured according to NF P94-051. All soil characterization results are summarized in Table 2. Density of the six soil range from 2575 kg/m3 to 2821 kg/m^3. Particle size distributions are plotted in a texture triangle (Fig.1), and confirm that the collected samples cover a wide range of natural variability. It is to be noted that REF and E5 exhibit a clay content higher than 60%, which is rare [17]. The six chosen samples, marked in red in Fig.1, cover a wide range of soils. The CEC of the samples under investigation ranges from 0.5 to 22.3 cmol+.kg^{-1}. Dividing these values by the clay fraction (below 2µm) leads to clay activities A_{CEC}, ranging from 6.7 to 117.8 cmol+.kg^{-1}. The plasticity index of the samples goes from 11 to 32. E1 sample is too sandy to carry out Atterberg limits.

	REF	E1	E2	E3	E4	E5
Effective particle density (kg/m^3)	2661	2714	2821	2810	2806	2575
CEC (cmol$^+$.kg^{-1})	14	4	5	7	13	21
A_{CEC}	28	39	20	14	34	118
Liquid limit (%)	53	-	43	58	51	58
Plastic limit (%)	27	-	29	37	19	47
Plasticity Index	26	-	13	21	32	11

Table 2 *Geotechnical parameters of the six soil samples.*

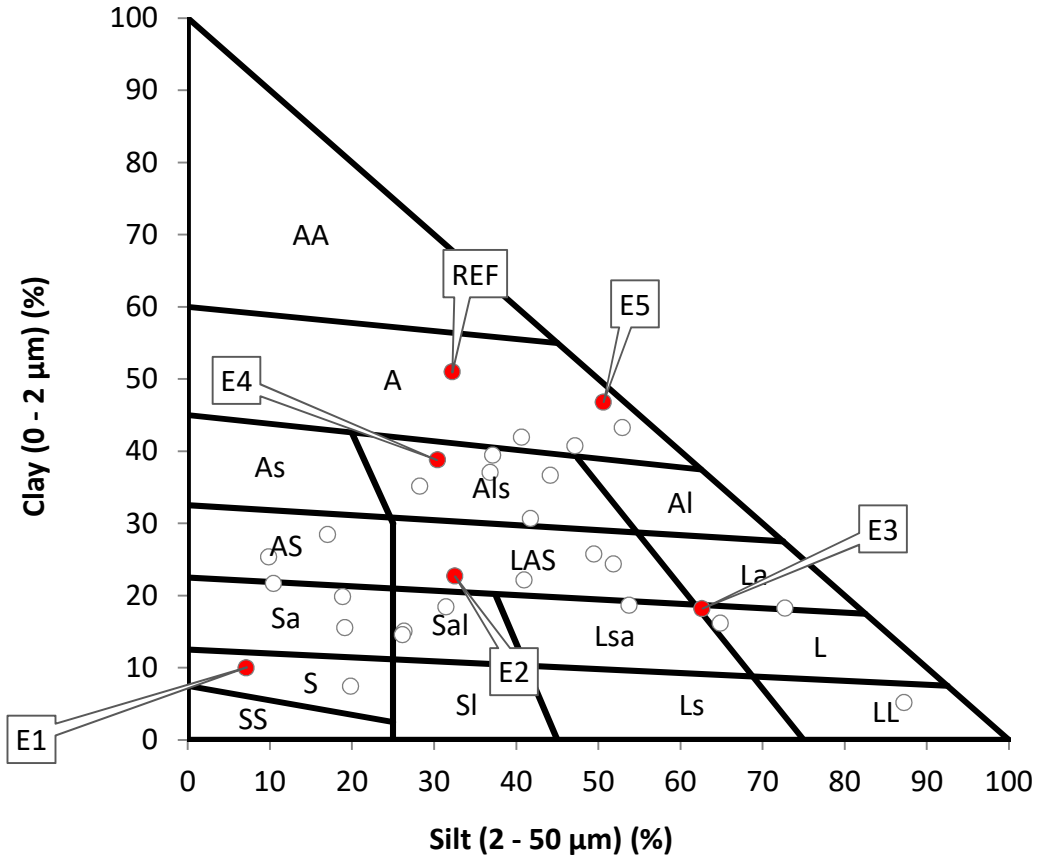

125

Fig.1 *Clay silt and sand distribution of the 27 collected soil samples. The six red dots correspond to the six samples selected for slip making and rheological studies*

126 # 2-2- Earth slip preparation

127 Raw samples at natural water content were prepared as follow:
128
129 1. Earth was mixed with a small quantity of water (mass ratio of about 1 water for 1 of raw earth);
130 2. The mix was blended with a paddle mixer for 5 minutes;
131 3. The slip was sieved with a 2 mm square sieve (a mesh size commonly used by builders working
132 with hemp-earth);
133 4. The slip was kept at rest for 24 hours in order to ensure the dilution of all earth clumps;
134 5. It was then blended again with a paddle mixer for 1 minute;
135 6. The water content was measured by oven drying (at 105°C, up to weight stabilization,
136 according to XP CEN ISO/TS 17892-1).
137
138 The first earth slip, with a controlled water content, was then progressively diluted with water to vary
139 the rheological behavior by controlling the water content.

140

III Rheology measurement methods

3-1- Rheometer

For the experimental validations, the yield stress values were measured using a rheometer with vane geometry. The mixtures were poured into a cylindrical container and vigorously mixed by hand to avoid thixotropy, segregation, and bleeding effects. The slip temperature was measured just before each test. These precautions were taken to avoid the measurement bias that could be due to temperature variations, sedimentation, or the structural build-up that occurs in the slips at rest. The yield stress was measured using an Anton Paar Rheolab QC rheometer equipped with vane geometry (four-bladed vane – 6 cm in height and 4 cm in diameter). The measurement procedure was similar to the one used in [43], [44]. A strain growth was applied to the sample at a shear rate of 0.01 s^{-1} for 400 s. At such a low shear rate, viscosity effects are negligible, and the yield stress can be computed from the measured torque peak value at flow onset. Each yield stress measurement was performed three times to ensure procedure reliability. The curves obtained show a classical stress growth evolution.

3-2- Slump / spreading flow test

The slump flow/spreading flow test is widely used in the construction industry to assess the workability of cementitious mixtures. It involves pouring and compacting the paste into a container (Fig. 2) using a standard procedure and measuring the slump or the spreading diameter to estimate the workability of the slip [45], [46]. The most commonly used geometries for these tests are the ASTM Abrams cone (H_0 300mm, R_{0max} 100mm, R_{0min} 50mm) and the ASTM minicone (H_0 50mm, R_{0max} 50mm and R_{0min} 35mm). For fluid pastes such as earth slips, a cylindrical container can also be used. In the present study, both the cylinder and the cone were tested, with different aspect ratios and volumes:

- a cylinder with a radius R_0 of 27mm and a height H_0 of 90mm, for a volume V of 0.206 dm^3 and an aspect ratio of 1,67;
- a cone with H_0 =150mm, R_{0max} =100mm, R_{0min} =50mm, for a volume V of 2.75 L and an aspect ratio around 2.

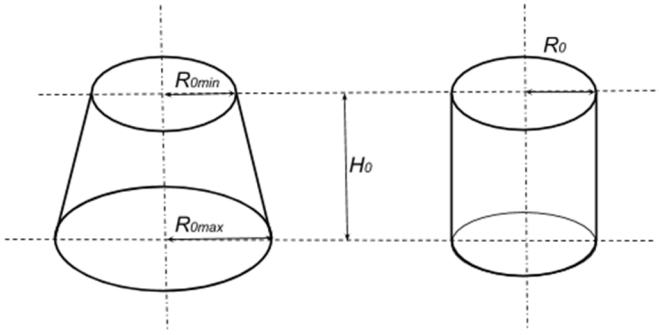

Fig. 2 *Initial shapes for the slump/ spreading flow test*

Theoretical framework

An analytical relationship exists between the slump and the yield stress of a granular suspension [47], [48]. Four cases can be observed when lifting the container:

- No slump: there is a critical yield stress of the paste for which no slump occurs. Theoretically, if we assume that the paste should undergo a pure elongation deformation and that the Von Mises yield criterion is applied, this critical yield stress is equal to $\sqrt{3}\rho g H_0$, namely a dimensionless yield stress $\tau'_0 = \frac{\tau_0}{\rho g H_0} = \sqrt{3}$. It was confirmed by the numerical simulations and experimental results of Roussel and Coussot on the ASTM Abrams cone and the ASTM minicone [48]. Above this critical yield stress, the paste is too rigid to yield under its own weight, and this kind of experiment is not appropriate. In this case, a squeeze flow [49] or a dropping cylinder test [30] could be used to enforce the deformation.

- Slump flow, with no spreading: the final shape is close to the initial one, the stress and strain variations in the radial direction are small, yielding to a slightly barreling final shape. In this case, by considering a pure elongation flow, Roussel and Coussot [48] and Pierre, Lanos and Estellé [47] apply a Von Mises criterion to the paste, which leads to the following analytical expression for yield stress τ_0 as a function of the slump value S (or of the final height H):

$$\tau_0 = \frac{\rho g H}{\sqrt{3}} = \frac{\rho g (H_0 - S)}{\sqrt{3}} \qquad (1)$$

  This theoretical expression is valid only with the assumption of a high initial height compared to the initial radius of the sample. Roussel and Coussot [48] show that it is accurate for a dimensionless yield stress $\tau_0{}'$ that ranges between 0.45 and $\sqrt{3}$, i.e. a dimensionless slump $S' = \frac{S}{H_0}$ lower than 0.1.

- Spreading (pure shear flow, with final height H << final spreading radius R): in this case, Roussel and Coussot [48] propose a formula relating the yield stress and the spreading distance (radius R):

$$\tau_0 = \frac{225 \rho g V^2}{128 \pi^2 R^5} \qquad (2)$$

  with V the volume of water, ρ its density and R the final radius of spreading

- Spreading, with a remaining cone or cylinder (mix of slump flow and spread regime): Pierre, Lanos and Estellé [47] propose an analytical formulation for this intermediate regime. They assume that the upper part of the deformed sample, which they call “hat”, and the central zone of the lower part are subjected to elongation flow only (Eq.2). Inversely, they apply a pure shear flow theory to the spreading zone of the lower part, which leads them to resolve a second order polynomial equation and to take its positive solution:

$$\tau_0 = \left(\frac{-b + \sqrt{b^2 + 4 a V_0}}{2a} \right)^2 \qquad (3)$$

With:

$$a = \frac{\pi {R_0}^2 \sqrt{3}}{\rho g}$$

$$b = \left[\frac{8\pi}{15}(R - R_0)^{5/2} + \frac{4\pi}{3}R_0(R - R_0)^{3/2} + \pi {R_0}^2(R - R_0)^{1/2}\right]\sqrt{\frac{2}{\rho g}} \quad (4)$$

Experimental method

Apart from slip variabilities, the different parameters investigated in this study are as follows:

1. Geometry of the container: as presented above, two geometries are examined: a cone and a cylinder, very different in volume and aspect ratio.
2. Surface roughness: according to Roussel [48], the wetting angle of the material on the solid surface affects the measured yield stress. Improving the wetting of the surface (getting ϑ close to zero) could theoretically provide an infinitely small yield stress measure. Furthermore, some sliding could occur at the interface, due to the well-known lubricant property of muddy suspensions. In order to examine these possible phenomena, two instances of surface roughness were tested, one with sand-paper, the other with melamine wood.
3. Calculus method: two methods are available in the literature for yield stress measurement by spread test [47], [48]. Both were applied to cementitious materials. In the present study, these two methods are assessed for earth slips.

3-3- Dipping test

The plate cohesion meter was developed in the 1980s by Lombardi for cementitious materials [50]. It involves a square metal plate, fitted with a balance that measures the weight of the paste remaining on the plate surface after soaking. Sonebi, Svermova and Bartos [41] use it on cement slurries to complement the test with a rheometer and do not use a cohesion parameter such as yield stress. However, through knowledge of the mass *M* and the plate area *A*, a yield stress could theoretically be estimated:

$$\tau_0 = \frac{Mg}{A} \quad (5)$$

In practice, the results are varied: when the plate emerges from the mixture, some tensile stress and flowing exist on the inside/outside interface. Hence, Eq.5 is no longer valid.

In the present study, to improve this experimental device in order to properly estimate the yield stress, the tool was weighed with a 10N force sensor all the way from immersion to its complete exit from the slip (Fig. 3.I). Thus, the validity range of the test depends on the test design. In the present case, the upper limit is given by the force sensor capacity, leading to a maximum measurable yield stress of 100 Pa. Thus, the main difference with the work of Sonebi, Svermova and Bartos [41] is that in the present case, a little actuator lifts the plate, at a rate of 2.5 mm/s, up to a complete exit. At the beginning of the experiment, the slip is vigorously mixed by hand to avoid build-up and the sedimentation bias, the force transducer is tared to cancel the proper weight of the plate, and the plate is immediately immersed. Then, the motor starts raising the plate. The force transducer measures only an apparent weight of matter, renamed *W',* which opposes the rise of the sheet ($W' = W + buoyancy - gravity$). In addition, we developed a cylindrical sheet rather than a plane geometry to increase the contact surface (and the accuracy of the results), and we stuck rough sandpaper on its surface to ensure that the shearing occurs into the slip and not at the sheet walls (Fig. 3.II). The cylindrical sheet is 100 mm in height, 150 mm in diameter, with a thickness of the steel sheet plus sandpaper of 4 mm.

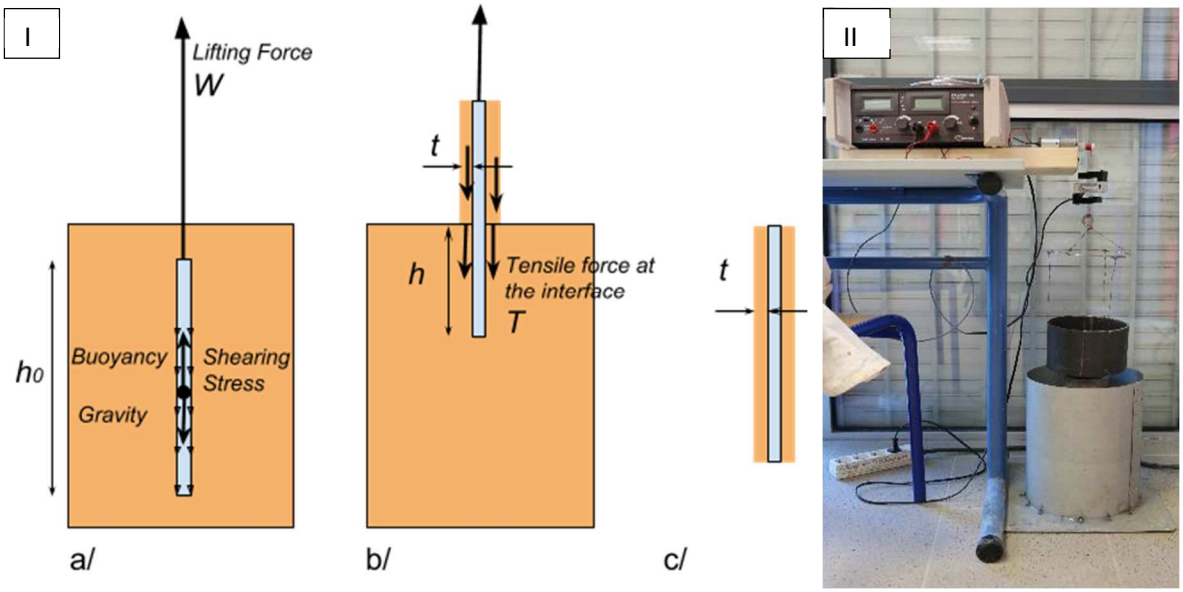

Fig. 3 *I) The dipping test: a/ initial state; b/ device partially emerged; c/device totally out. II) The experimental device developed for the "plate" test*

The theoretical frame is the same as for the plate test of Amziane, Perrot and Lecompte [51]. Three distinct phases have to be taken into consideration (Fig. 3I):

- The cylinder is totally immersed:

In this case, the slip shearing stress is the only apparent load:

$$\tau_0 = \frac{W + \rho g V_0 - M_0 g}{A_0} = \frac{W'}{A_0} \qquad (6)$$

With A_0 , V_0 and M_0 respectively the sheet area, volume, and mass and ρ the density of the slip.

- The cylinder is partially out:

The immersed part bears the same shearing load as in the first case, and the outer part bears the weight of the slip remaining on the surface. Additionally, the buoyancy of the outer part of the plate no longer exists, and a tensile force at the inside/outside interface opposes the rising of the device:

$$W = \frac{\tau_0 A_0 h}{h_0} + \rho g t A_0 \left(1 - \frac{h}{h_0}\right) + T - \rho g V_0 \frac{h}{h_0} + M_0 g \qquad (7)$$

$$W' = \frac{\tau_0 A_0 h}{h_0} + \rho g t A_0 \left(1 - \frac{h}{h_0}\right) + T + \rho g V_0 \left(1 - \frac{h}{h_0}\right) \qquad (8)$$

With h_0 the height of the sheet, h the immersed height, t the thickness of the slip remaining on the outer part, ρ the slip density and T the tensile force at the inside/outside interface. In a first approximation, this tensile force is estimated by considering a simple Von Mises yield criterion:

$$\mathrm{T} = 2\sqrt{3}\tau_0 \mathrm{t} p_0 \qquad (9)$$

With p_0 the perimeter of the cylinder.

It yields an analytical estimation of the slip yield stress when the cylinder is partially out:

$$\tau_0 = \frac{W' - \rho g\left(1 - \frac{h}{h_0}\right)(V_0 + tA_0)}{A_0\frac{h}{h_0} + 2\sqrt{3}\tau_0 t p_0} \qquad (10)$$

- The cylinder is totally out:

We weigh the slip remaining on the cylinder surface, and we add the buoyancy effect that no longer acts. As for the plate cohesion meter, we can deduce the mean remaining thickness *t* using this measurement and the density of the slip:

$$t = \frac{W - M_0 g}{\rho g A_0} = \frac{\frac{W'}{\rho g} - V_0}{A_0} \qquad (11)$$

Where A_0 and V_0 are respectively the sheet area and volume, and ρ is the density of the slip. As previously explained and shown by Maillard et al. [52], this thickness cannot be directly related to the yield stress of the fluid. Gravity and the viscous effects stemming from the sheet velocity and eventually the capillary effects yield to other analytical formulas for *t*. Maillard et al. [52] find that, roughly, the thickness *t* at low velocities and few capillary effects (yield stress higher than 25 Pa) may be expressed for yield stress fluids as:

$$t \approx 0.3\ \frac{\tau_0}{\rho g} \qquad (12)$$

That is less than one third of the maximum thickness that the sheet could theoretically raise. This equation is confronted to results in the next paragraphs.

The measurements of force and position of the cylinder relative to the mixture surface are used to compute the yield shearing stress when the sheet is totally or partially immersed. Fig. 4 shows results with the raw data W' and the estimation of the yield stress using Eq.6, Eq.7, and Eq.10.
The different parameters of the test are found mainly in the calculation method. In order to choose a yield stress value, the two first phases are analyzed:

- The first phase curve is close to a vane rheometer measure: an elastic phase and then a plastic phase with a maximum are observed.
- The second phase shows a variable yield stress value. It seems that the edge effect at the fluid/air interface is not negligible and affects the measurement.

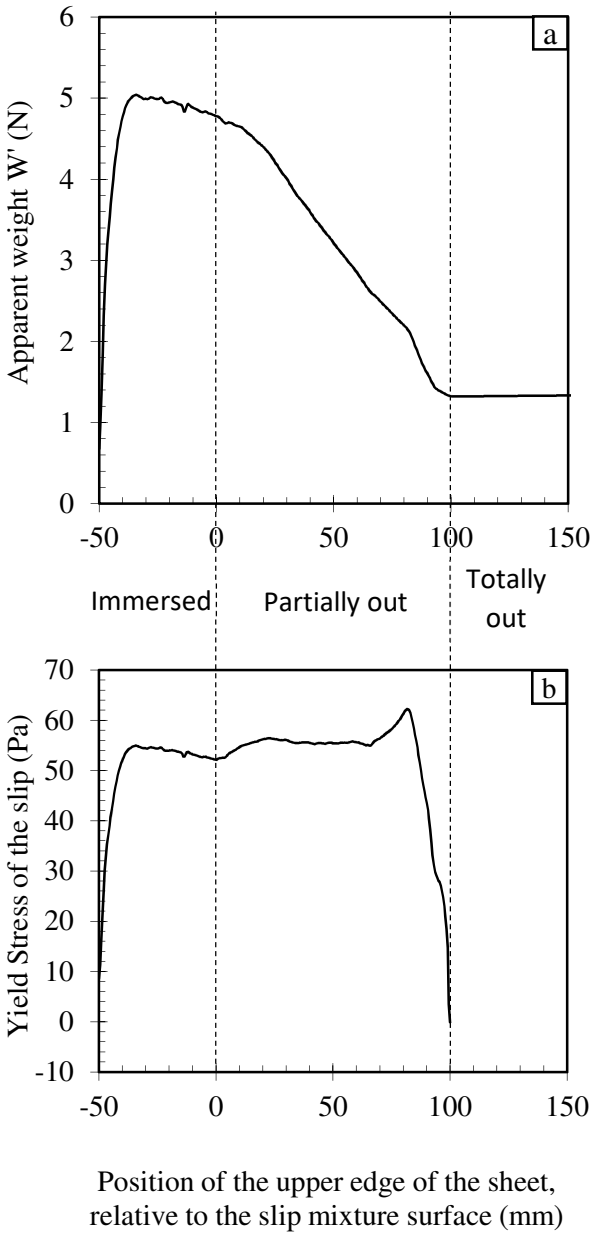

306

307

Fig. 4 *Typical results of "Dipping test" measurements (a): raw data, (b): yield stress estimation*

308

309 # 3-4- Rough wall cone

310 The inclined plane test was proposed by Coussot and Boyer in the 1990s [34], [53] to examine the
311 possibility of predicting the free surface flow characteristics of non-Newtonian fluids such as mud and
312 clay-water mixtures. Theoretically, it involves an infinite plane slope on which a mixture is poured
313 slowly enough to avoid the effects of inertia and to obtain a uniform height of material. Practically, an
314 approximately steady flow of mixture is imposed on a given slope and progressively stopped.
315 Considering the no-wall slip at the surface of the device, a simple momentum balance leads to a yield
316 stress calculation.

In order to ease the on-field use of such a test, a new test was designed and inspired from viscosity cones. The main asset of a cone, compared to a plane, is that the slope is imposed by its shape. This test was designed for this study and called the "rough wall cone test". All the geometry parameters are described in Fig. 5 (Left). A yield stress measurement is obtained from the following steps:

- Filling in a cone preliminarily fitted with rough sandpaper and closed at the lower part;
- Then, freeing the lower part and letting the fluid drop;
- Weighing the remaining fluid when the flow stops (Fig. 5, Right).

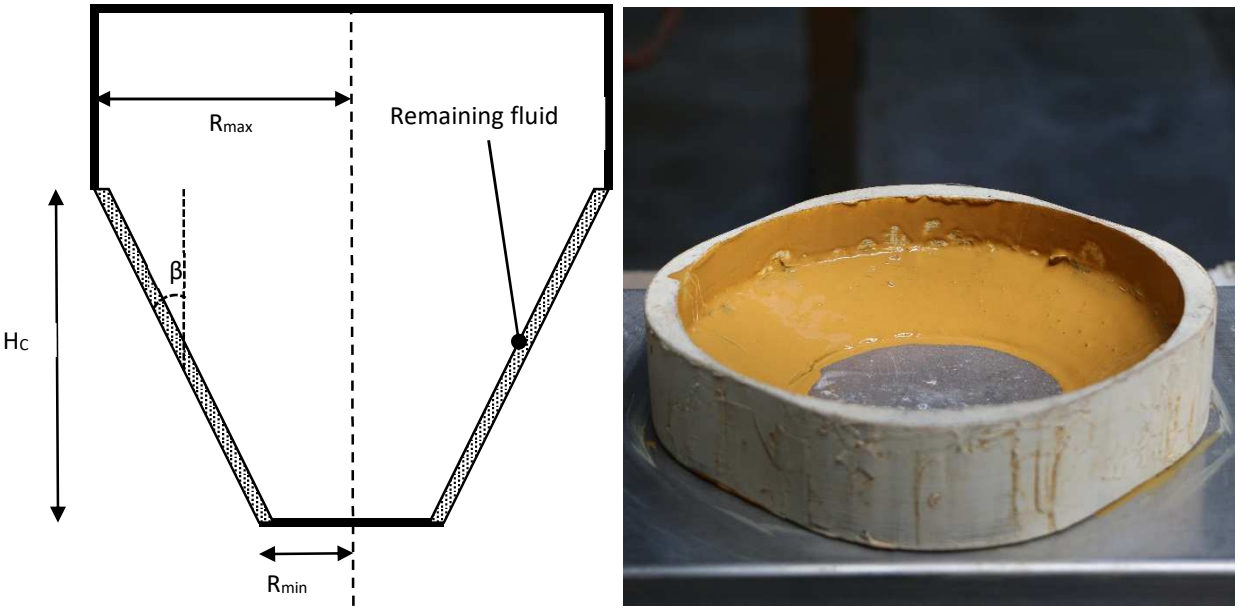

Fig. 5 *Left : Cone geometry parameters ; Right : Remaining slip on cone surface after testing*

If we use a large cone, i.e. $R_{min} > (R_{max}-R_{min})$, with a very obtuse angle, we can assume that the flow is slow enough to avoid viscous effects, to be in a quasi-steady state, and that the initial fluid thickness is close enough to the equilibrium thickness to limit the surface tension effects. Then, the momentum balance can easily be deduced, as for the inclined plane (Eq. 13) when the flow stops:

$$\tau_0 = Mg\frac{cos\beta}{A_{cone}} = \frac{Mgcos\beta}{\pi(R_{min}-R_{max})H_C} \qquad (13)$$

3-5 Marsh funnel and viscosity cups

Other devices sometimes recommended for earthen constructions are the viscosity cones, such as the Marsh funnel, or the viscosity cups. The test generally involves measuring the flow time necessary to empty the cone. This time corresponds to the fluidity of the material, which can generally be related to its viscosity [39]. The aim of the present study was to estimate not the viscosity of the fluid, but its yield stress. For yield stress fluids with a yield stress above 12.5 Pa, the Marsh funnel does not empty entirely. In this case, Balhof et al. [35] give a formula to estimate the yield stress using the remaining static height of fluid in the device (Fig. 6 and Eq.13). The authors assume that the tangential stress is sufficiently low in the cone part to let the fluid slip and that there is no slipping at the cylinder wall. This assumption, considering that the flowing mode only depends on the geometry of the wall, seems

quite strong. Hence, the Marsh funnel (4.76 mm and 8 mm opening) and flow cups (3, 4, 5, 6 and 8mm) were also tested.

$$\tau_0 = \frac{\rho g(h_s+L)}{2\left(\frac{L}{R}+\frac{H_F}{R_F}\right)} \qquad (13)$$

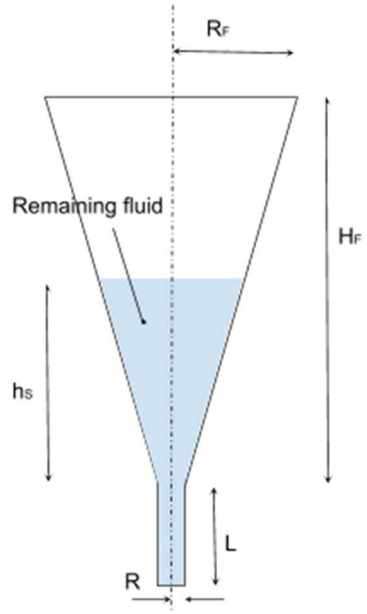

Fig. 6 *Marsh funnel geometry*

IV Experimental results

Rheometer measurements can only be carried out in laboratory conditions. As this tool is designed and used to give precise and accurate results, it was chosen as a reference to evaluate the accuracy of the other tests.

First, to examine the effect of soil variability, several slips were prepared with each of the six different soil samples by varying their water content. Apart from rheometer measurements, the yield stress measures range from 0 to 250 Pa, depending on the water content and raw earth cohesion. Then, following results will be plotted according to this range. Second, the following sections present the design and calculus parameters of each test alongside characterization results, in order to assess the suitability of the different tests.

.

4.1 Rheometer

In order to understand the variable rheological behavior of earth, an observation of the yield stress versus water content results is needed. **Fig. 7** presents these results within a yield stress range of 0 to 100 Pa. E1 shows a short evolution of the yield stress with a zero value close to a water content

of 1. At the opposite, E3 reach a yield stress of zero at a water content higher than 3. Most of the earth show similar curve shapes, but at different water content. Thus, the graph shows an important variation of cohesive behavior.

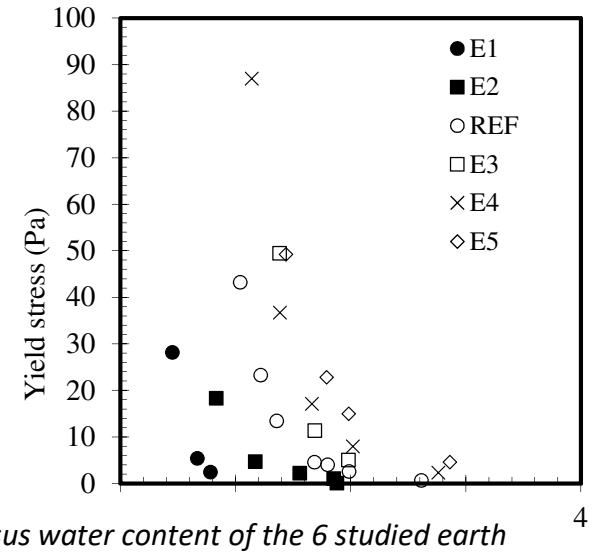

***Fig. 1**: Yield stress versus water content of the 6 studied earth*

Attention was paid to the limits of vane geometry. Pierre et al. [54] define a ratio v that indicates the vertical stability/instability position in relation to the shear surface described by the vane tool in rotation:

$$v = \frac{1}{h_c}\frac{\sqrt{3}\tau_0}{\rho g} \quad (15)$$

With h_c the vane tool height, τ_0 and ρ resp. the paste yield stress and its density.
If this ratio is close to or higher than 1, then the tested material is too stiff to flow. Moreover, if the tested earth has a swelling behavior, empty spaces around the tool can appear. To analyze the robustness of rheometer measurements, the recommendations of Pierre et al. [55] were used. The tested slips show yield stresses going from about 0 to about 850 Pa, with solid volume fractions evolving from 0.11 to 0.8. The v ratio was calculated for every rheometer measurement. Fig. 8 shows the evolution of this ratio versus the measured yield stress. Regardless of the earth type, the limit of v =1 is reached for a yield stress of 495 Pa. The analysis of the rheometer data confirms this phenomenon: under 495 Pa, the maximum standard deviation is 5% and above 495 Pa, the standard deviation can reach 95%.

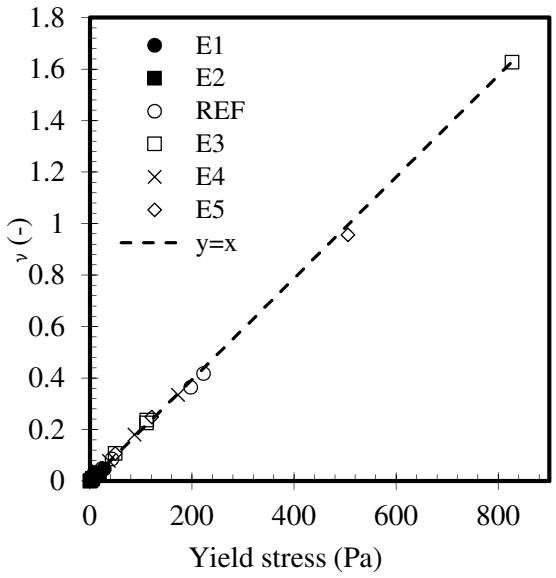

Fig. 8 *ν Ratio vs. vane tool yield stress measures*

4.2 Slump flow and spreading flow

Influence of the apparatus design

The effect of geometry and surface roughness were tested on the reference slip. The raw data were treated according to Pierre et al. formula (Eq.3 & Eq.4). Results are presented in Fig. 9a.
First, the roughness of the surface does not affect the results: the matter flows of itself and sticks to the surface, even if clay pastes are known to act as a lubricant, even on a very smooth spreading surface. In contrast, the initial geometry of the sample showed a considerable influence on the measurements. It appears that the cone results match the rheometer values well between 0 and 50 Pa, whereas the cylindrical container seems to induce a divergence. Two parameters are involved in the influence of geometry: the volume and the shape of the container. Clayton et al. [56] tested the influence of these parameters on the slump of pigment pastes and mineral pastes and compared their results to those of the literature on clay pastes. They show that there is no influence of the shape (conical or cylindrical) on the slump, but when varying the heights with an aspect ratio of 1, they observe the strong influence of the volume of the container. How the volume affects the measure can be estimated through the limit of representative dimensions of the final spread. In this case, the limitative dimension is the final height *H* of the spread fluid, and the criteria can write as follows: $H>k\emptyset_{max}$ with $\emptyset_{max}$ the maximum particle diameter of the granular suspension and k the number of particles in the thickness for which the fluid remains representative. Generally $k \approx 6$. Considering a total spreading, we can rewrite the Roussel equation (Eq.2) in terms of the minimum volume:

$$V > \left(\frac{225\rho g}{128\,\tau_0}\right)^2 \pi(k\emptyset_{max})^5 \qquad (16)$$

Fig. 10 shows the container volume that should be aimed to measure a yield stress of 2 Pa and 10 Pa, as a function of the desired final fluid height. For the cylinder under investigation ($V_{cylinder}$=0.21L), a 10 Pa yield stress is hardly measurable as the final height will be 6mm (i.e. three maximum diameters of the slip particles), while for the cone (V_{cone}=2.75L) H should be higher than 10 mm. For such suspensions, with very low yield stress and containing quite coarse particles, a minimum volume of the container must be considered and is discussed below.

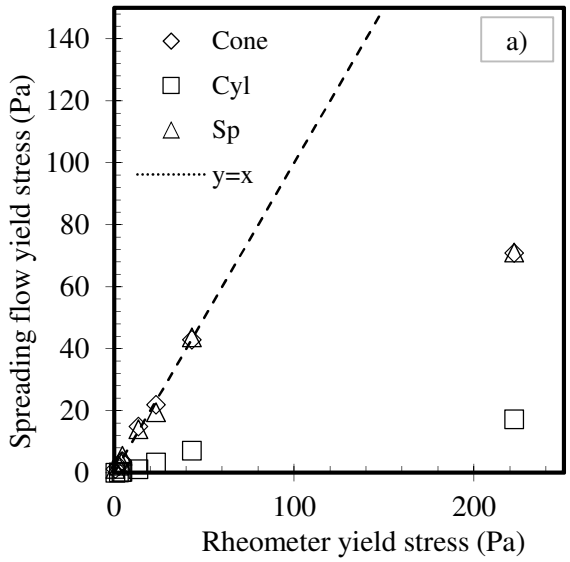

409

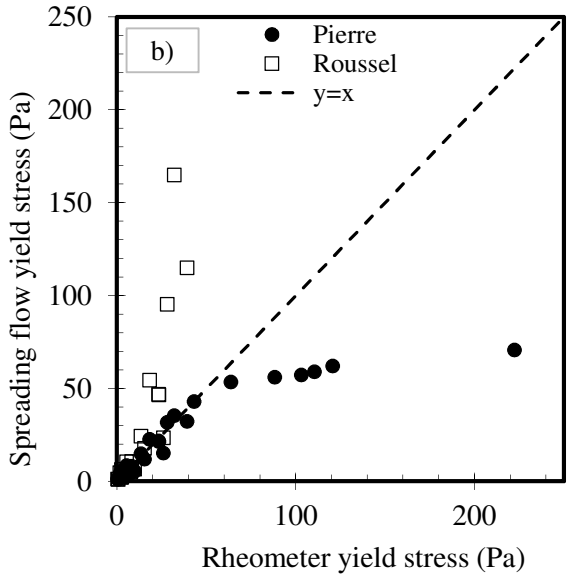

410

Fig. 9 *a) Yield stress of one slip measured by spreading on sandpaper (Sp) or melamine wood, using a cone or a cylinder (Cyl), using Pierre et al.'s calculus compared with rheometer measurement. b) Yield stress of the six different slips measured by spreading*

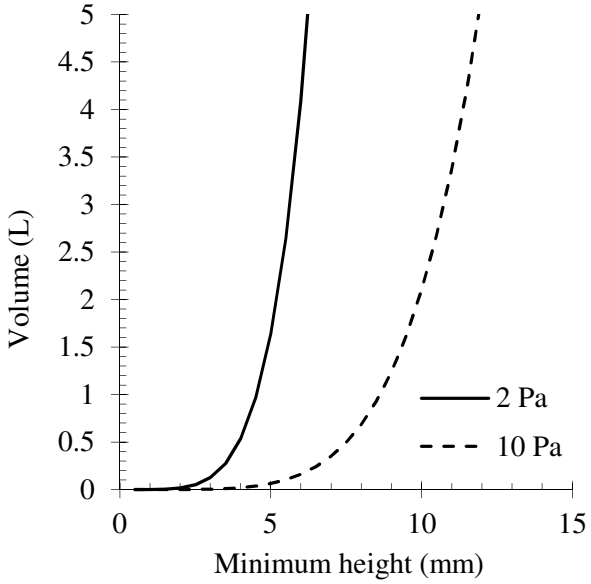

Fig. 10 *Container volume for the spreading test according to a minimum height at the end of the spreading test*

The aspect ratio and the initial height of the container could also affect the results, due to inertia effects. Roussel et al. [48] indicate that the yield stress must remain higher than the inertia ($I = \rho\left(dR/dt\right)^2$) during the flow to avoid abrupt liquid–solid transitions. Then, the flow speed can be influenced by the height of the sample and the yield stress itself. A video analysis was conducted on two different slips and with cylindrical and cone containers to measure flow speeds. The results are given in Table 3. The $I<\tau_0$ criterion is not met for low yield stress, regardless of the container, which can explain the discrepancies for very fluid suspensions and stresses the differences due to the volume of the container.

		τ_0=62Pa	τ_0=0,5Pa
Density (kg/m^3)		1330	1285
Average radial speed (m.s^{-1})	Cone	0.16	5
	Cylinder	0.06	20
Inertia (Pa)	Cone	34.2	243
	Cylinder	5.4	500

Table 3 Inertia during spreading of two slips

Influence of data processing

Fig. 9b presents the yield stress calculated from spreading tests with the Pierre et al. formula [47] and the Roussel et al. formula [48]. The results with the Pierre et al. calculation method have a validity range going from 0 to about 50 Pa, while results with the Roussel et al. calculation method have a smaller validity range going from 0 to about 25 Pa. Roussel and his coworkers assume that all the material spreads by pure shearing, which is not true above 20 Pa. Above this value, the Roussel et al. formula overestimates the yield stress.

Standard deviations have been calculated, but are not observable on this representation (Fig. 9b), showing very good repeatability of the results. Average errors between the flow and

rheometer measurements have been estimated within the validity range expressed above. It appears that these errors depend on the soil type: E1, E2, and E4 (respectively 34%, 56%, and 43% of average errors) slips show an average error higher than REF, E5 and E3 (respectively 19%, 5% and 14%).

4.3 Dipping test

The first phase, i.e. when the cylinder is totally immersed, provides the most reliable results, as the calculus does not take into account the surface tension the thickness measurements of the remaining slip measurements. As presented in Fig. 11, the first phase results are in line with the rheometer measurements. Depending upon the soil type, average errors go from 18% to 51%. The highest errors are not found for the highest yield stress measurements. Nevertheless, errors can be caused by a non-continuous shear surface, as expressed before for the vane tool. When the slip is too stiff, empty spaces can be created while the cylinder is lifted.

Second phase results, when the cylinder is partially out, always show an overestimation or an underestimation of the yield stress. A slight inclination of the cylinder directly influences the estimation of the mass of remaining slip on the cylinder and the surface tension effect.

Then, Fig. 11 also presents results of a yield stress calculation based on the third phase, when the cylinder is totally out of the slip. According to Maillard et al. [52], there should be a proportionality coefficient between the thickness of the remaining material on the cylinder and the real yield stress (Eq. 12). In the present case, this model does not fit the experimental points. Taking all the results into account, the proportionality coefficient is 0.66 with a very large total standard deviation (1.22).
In the same study [28], a more precise model estimates the thickness during the "partially out" phase:

$$t = \frac{\lambda}{2} - \frac{\alpha \rho g \lambda^2}{3\tau_0} \qquad (15)$$

With t the thickness of the remaining material after the test, λ the thickness of the sheared material in the air-material interfacial zone, α a fitting factor and τ_0 the material yield stress.
In the case of earthen material, the thickness of the sheared material (λ) depends on the particle size distribution and clay activity of the tested material. The coarser the aggregates are or the more cohesive the clay is, the larger this sheared zone will be. The differences of granular distributions and the cohesiveness of the six slips of this study explain the high discrepancies of the results.

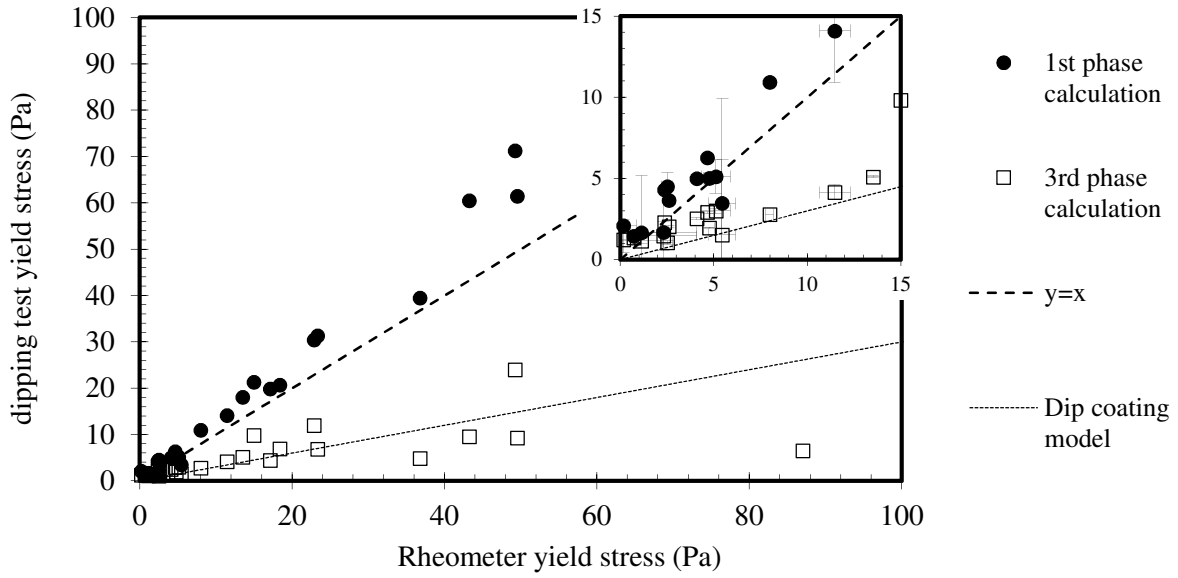

Fig. 11 *Yield stress of the six different slips measured using the dipped cylinder test, from the 1st and 3rd phase of the test compared with the rheometer measurements. The 3rd phase results are compared to the dip coating model of Maillard et al. [28]*

4.4 Rough wall cone

Fig. 12 shows the results of the yield stress measured using the rough wall cone for the six different slips and three different cone designs (see Fig. 6):

- β=60°- cone with a cylindrical upper part
- β=60° - cone without a cylindrical upper part
- β=85°- cone without an upper part

For every cone R_{min}=6 and R_{max}=10

The β=60°-cone with a cylinder upper part provides results in line with the rheometer measurements, regardless of the soil type. The upper limit in terms of yield stress is 230 Pa, above which no flow occurs. Around a yield stress of 200 Pa, results are disputable as there is no real flow occurring but a pure shearing of the central part of the sample. In addition, important errors are observed between 0 and 3Pa, where the yield stress measurements are highly overestimated. Because of the roughness of the cone wall, it is possible that coarse particles remain on the apparatus whereas they should have flown away. Then, the validity range of this test could go from 3 to 200 Pa. Within this range, average errors range from 8% to 58% depending on the soil type.

The other two designs do not give proper results. For the cone with β=85°, the slope is not high enough to induce a flow. Regarding the design without an upper part extension, Coussot et al. [34] describe the importance of a stopped flow and a constant thickness of the material on the apparatus. In their case (inclined plane slope), the flow would occur in 30 to 40 minutes. In our case, the flow stops a few tens of seconds after the cone has been lifted. Thus, the lack of material above the beginning of the slope induces a non-continuous thickness of the flowing material. This phenomenon leads to a highly underestimated yield stress.

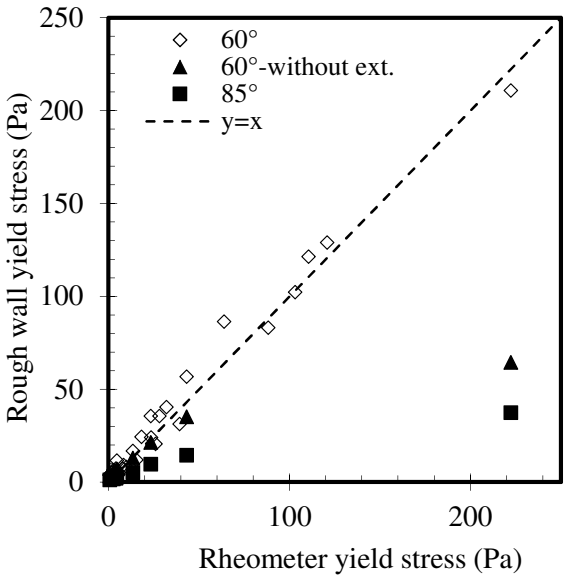

494

Fig. 12 *Influence of the test design on cone yield stress measurement compared to rheometer measurements. The six earths were tested on the β=60° cone, while only REF was tested on the β=85° cone and the cone without extension*

495 4.4 Marsh funnel and viscosity cups

496 The earth slips were also tested using the Marsh funnel and viscosity cups. First, these two
497 tests are designed for viscosity measurement. The formula developed by Balhof et al. [35] was
498 used to treat the Marsh funnel results. For the two tested openings, results show an important
499 overestimation of about one order of magnitude. Furthermore, there are only one or two
500 water contents at which the test works, in the range 12Pa-25Pa of yield stress for the standard
501 funnel flow geometry. Outside these limits, the slip does not flow at all or flows completely
502 through the device. We observed the same problems for the viscosity cups, with even less
503 cases where measures are possible.

504 V. Discussion

505 5.1 Comparison of yield stress measurement methods

506 Table 4 summarizes the advantages and disadvantages of any tests considered in this study.
507 Maximum measurement uncertainties are calculated from the sensors' accuracies and with
508 the different yield-stress formulas (Eq.3 to Eq.11). The maximum average error is defined as
509 the maximum of average differences for each water content and each soil type, between
510 rheometer measurements and the compared test.
511 Whereas the spread test and the rough wall cone test are directly usable on site, the dipping
512 test still requires adaptation. A proposal is presented in the following section. To compare the
513 validity range of each test, it is necessary to consider the required yield stresses for different
514 earthen construction methods:

- Light earth: knowledge about earth slips has been developed during this project. Following the know-hows of builders, earth slips with a yield stress between 2 and 80 Pa, according to the earth cohesive behavior, are considered to be valid.
- Earthen concrete: the same rheology as cement concrete is generally aimed at. For self-compacting earthen concretes, Ouellet-Plamondon et al. [33] defined an optimal yield stress between 200 and 500 Pa.

Test	Maximum measurement uncertainty (%)	Maximum error (%)	Validity range (Pa)	Advantages	Drawbacks
Rheometer	0.51	-	0 - 500 (with a 6 cm-in-height vane tool)	Sensitive, reference value	Laboratory apparatus, expensive and not adapted to field conditions
Spreading	0.2	56% - soil dependent	0-50	Fast and easy to process, very easy and cheap to design	Requires a plane and perfectly horizontal surface (not appropriate for earthen concretes); strong influence of the device volume
Dipping	0.05	51% - soil dependent	0-100	The most accurate test compared to rheometer; quite easy to process	First designed for the laboratory: a robust device has to be developed for field conditions; a large amount of slip is needed for the test; the data processing must be adapted to the device geometry (area).
Rough wall cone (β=60°- with extension)	0.2	58% - soil dependent	3-200	Fast and easy to process, more appropriate for high yield stress materials	The apparatus has to be machined or 3D printed, possibly user-dependent due to lifting rate and cone orientation
Marsh funnel and Viscosity cups	-	-	-	Easy to do and already used for other applications	Not appropriate for yield stress measurement of earth slips

Table 4 *Summary of the comparison of yield stress tests*

Measurement uncertainties are below the maximum average errors. Even if slips are mixed right before each test, for slips with coarse aggregates, sedimentation can occur before the test or the homogeneity of the slip can be impacted by the flow. Then, particle size distribution, clay activity, and particle swelling capacity could affect the results. Nevertheless, the maximum errors compared to reference values is sufficient for application in field conditions in the case of the spreading, dipping and rough-wall cone tests (β=60°-with extension).

Fig. 13 shows the modelling of the experimental results showed in **Fig. 7** (without E5 which shows an evolution close to REF), following an exponential fitting. This abacus allows to quantify how much water should be added or removed to reach a targeted yield stress.

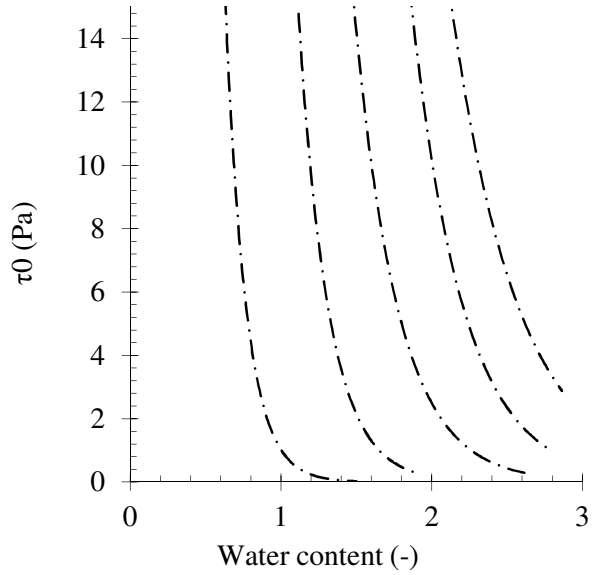

***Fig. 13**: Modeled yield stress versus water content of 5 earth*

VI Conclusions

This paper aims to demonstrate the possibility of measuring the rheological behavior of an earth suspension with simple tests. Firstly, the six earth chosen for sample manufacturing are representative of the large natural variability of 27 collected earth from Normandy and Brittany regions. With the six selected earth, different slips are manufactured with varying water contents. Soil suspensions behave like yield stress materials. Thus, their cohesive behavior is studied through the measurement of their yield stress. To do so, six different tests, of which two have been developed for this study, are compared: rheometer, spreading test, dipping test, rough wall cone, Marsh cone tests and viscosity cups.

Rheometer measurements were used as the reference, in a yield stress range between 0 and 500 Pa. Results can be summed up as follows:

- The six earth are very different in their geotechnical characteristics. Six different rheological behaviors are observed. Particle size distribution, clay activity and specific density affect the link between water content and yield stress;
- Marsh cone tests or viscosity cups are not adapted to the yield stress range of earth slips;
- Spreading test, dipping test and rough wall cone β=60°-with extension- gave satisfactory results respectively from 0 to 50 Pa, 0 to 100 Pa and 3 to 200 Pa. For these three tests, a 50% maximum discrepancy was observed. All these tests are easy to transfer to field conditions.

555 Along with yield stress versus water content model, these tests allow to evaluate how much
556 water should be added or removed to reach a targeted yield stress. This quantitative approach
557 can be used to characterize earth slip in laboratory conditions for light earth studies or in fields
558 conditions.

559 Finally, rheological results discrepancy level is slightly earth dependent. Further studies might
560 investigate the link between the rheological behavior and the geotechnical characteristics of
561 earth.

562 Acknowledgment

563 Eco-Terra Project is possible thanks to the financial support of the Normandy Region, the French
564 state, the Fondation de France, the ADEME and the Bretagne Region. Earth characterization tests
565 have been performed thanks to INRA d'Arras and Alexis Cothenet (IFSTTAR, Nantes). Rheology tests
566 were developed thanks to the help of Hervé Bellegou (IRDL, Lorient).

References

[1] J. E. Aubert, P. Maillard, J.-C. Morel, and M. Al Rafii, 'Towards a simple compressive strength test for earth bricks?', *RILEM*, 2015.

[2] M. Moevus *et al.*, 'Earthen construction: an increase of the mechanical strength by optimizing the dispersion of the binder phase', *Mater. Struct.*, vol. 49, no. 4, pp. 1555–1568, Apr. 2016.

[3] A. Arrigoni, C. Beckett, D. Ciancio, and G. Dotelli, 'Life cycle analysis of environmental impact vs. durability of stabilised rammed earth', *Constr. Build. Mater.*, vol. 142, pp. 128–136, Jul. 2017.

[4] K. K. G. K. D. Kariyawasam and C. Jayasinghe, 'Cement stabilized rammed earth as a sustainable construction material', *Constr. Build. Mater.*, vol. 105, pp. 519–527, Feb. 2016.

[5] F. Pacheco-Torgal and S. Jalali, 'Earth construction: Lessons from the past for future eco-efficient construction', *Constr. Build. Mater.*, vol. 29, pp. 512–519, Apr. 2012.

[6] F. Volhard, *Construire en terre allégée*. Actes sud, 2016.

[7] 'Marcom - Le terre-paille est une technique inégalable en in.pdf'. .

[8] T. Vinceslas, T. Colinart, E. Hamard, A. H. de Ménibus, and T. Lecompte, 'LIGHT EARTH PERFORMANCES FOR THERMAL INSULATION: APPLICATION TO EARTH-HEMP', p. 7, 2017.

[9] M. Degrave-Lemeurs, P. Glé, and A. Hellouin de Menibus, 'Acoustical properties of hemp concretes for buildings thermal insulation: Application to clay and lime binders', *Constr. Build. Mater.*, vol. 160, pp. 462–474, Jan. 2018.

[10] C. Niyigena, S. Amziane, and A. Chateauneuf, 'Multicriteria analysis demonstrating the impact of shiv on the properties of hemp concrete', *Constr. Build. Mater.*, vol. 160, pp. 211–222, Jan. 2018.

[11] E. Hamard, B. Lemercier, B. Cazacliu, A. Razakamanantsoa, and J.-C. Morel, 'A new methodology to identify and quantify material resource at a large scale for earth construction – Application to cob in Brittany', *Constr. Build. Mater.*, vol. 170, pp. 485–497, May 2018.

[12] S. Burroughs, 'Recommendations for the selection and stabilization of soils for rammed earth wall construction', in *11th International Conference on Non-cpnventional Materials end Technologies (NOCMAT, 2009)*, Bath, 2009, p. 9.

[13] S. Burroughs, 'Soil Property Criteria for Rammed Earth Stabilization', *J. Mater. Civ. Eng.*, vol. 20, no. March, pp. 264–273, 2008.

[14] D. Ciancio, P. Jaquin, and P. Walker, 'Advances on the assessment of soil suitability for rammed earth', *Constr. Build. Mater.*, vol. 42, pp. 40–47, May 2013.

[15] M. Hall and Y. Djerbib, 'Moisture ingress in rammed earth: Part 1—the effect of soil particle-size distribution on the rate of capillary suction', *Constr. Build. Mater.*, vol. 18, no. 4, pp. 269–280, May 2004.

[16] M. Hall and Y. Djerbib, 'Moisture ingress in rammed earth: Part 2 – The effect of soil particle-size distribution on the absorption of static pressure-driven water', *Constr. Build. Mater.*, vol. 20, no. 6, pp. 374–383, Jul. 2006.

[17] H. Van Damme, 'La terre , un béton d'argile', *Pour Sci.*, pp. 50–57, Jan. 2013.

[18] *NF P 94-056 - Analyse granulométrique par tamisage - Méthode par tamisage à sec après lavage*. AFNOR, Paris: Norme Française, 1996.

[19] *NF P 94-057 - Analyse granulométrique des sols - Méthode par sédimentation*. AFNOR, Paris: Norme Française, 1992.

[20] *NF P 94-051 - Détermination des limites d'Atterberg - Limite de liquidité à la coupelle - Limite de plasticité au rouleau*. AFNOR, Paris: Norme Française, 1993.

[21] *NF P 94-068 - Mesure de la capacité d'absorption de bleu de méthylène d'un sol ou d'un matériau rocheux - Détermination de la valeur de bleu de méthylène d'un sol ou d'un matériau rocheux par l'essai à la tache*. AFNOR, Paris: Norme Française, 1998.

[22] T. C. Major, J.J. and Pierson, 'Debris Flow Rheology ' Experimental Analysis of Fine-Grained Slurries Any rotating of fI imposed on the rotor [Van Wazer and mat . he . matical models of deb . ris flows have ! n length to the', *Water Resour.*, vol. 28, no. 3, pp. 841–857, 1992.

[23] J. D. Parsons, K. X. Whipple, and A. Simoni, 'Experimental Study of the Grain-Flow, Fluid-Mud Transition in Debris Flows', *J. Geol.*, vol. 109, no. 4, pp. 427–447, 2002.
[24] H. S. Kang and Y. T. Kim, 'Rheological properties of loose sands subjected to upward flow', *Can. Geotech. J.*, vol. 54, no. 5, pp. 664–673, 2016.
[25] P. Coussot and J. M. Piau, 'On the behavior of fine mud suspensions', *Rheol. Acta*, vol. 33, no. 3, pp. 175–184, 1994.
[26] S. W. Jeong, 'Grain size dependent rheology on the mobility of debris flows', *Geosci. J.*, vol. 14, no. 4, pp. 359–369, Dec. 2010.
[27] G. Azeredo, J.-C. Morel, and C.-H. Lamarque, 'Applicability of rheometers to characterizing earth mortar behavior. Part I: experimental device and validation', *Mater. Struct.*, vol. 41, no. 8, pp. 1465–1472, Oct. 2008.
[28] Q.-B. Bui, J.-C. Morel, S. Hans, and N. Meunier, 'Compression behaviour of non-industrial materials in civil engineering by three scale experiments: the case of rammed earth', *Mater. Struct.*, vol. 42, no. 8, pp. 1101–1116, Oct. 2009.
[29] A. Perrot, D. Rangeard, and A. Levigneur, 'Linking rheological and geotechnical properties of kaolinite materials for earthen construction', *Mater. Struct.*, vol. 49, no. 11, pp. 4647–4655, Nov. 2016.
[30] A. Perrot, D. Rangeard, and T. Lecompte, 'Field-oriented tests to evaluate the workability of cob and adobe', *Mater. Struct.*, vol. 51, no. 2, Apr. 2018.
[31] Z. Vryzas, V. C. Kelessidis, L. Nalbantian, V. Zaspalis, D. I. Gerogiorgis, and Y. Wubulikasimu, 'Effect of temperature on the rheological properties of neat aqueous Wyoming sodium bentonite dispersions', *Appl. Clay Sci.*, vol. 136, pp. 26–36, Feb. 2017.
[32] A. Perrot, D. Rangeard, and E. Courteille, '3D printing of earth-based materials: Processing aspects', *Constr. Build. Mater.*, vol. 172, pp. 670–676, May 2018.
[33] C. M. Ouellet-Plamondon and G. Habert, 'Self-Compacted Clay based Concrete (SCCC): proof-of-concept', *J. Clean. Prod.*, vol. 117, pp. 160–168, Mar. 2016.
[34] P. Coussot and S. Boyer, 'Determination of yield stress fluid behaviour from inclined plane test', *Rheol. Acta*, vol. 34, no. 6, pp. 534–543, 1995.
[35] M. T. Balhoff, L. W. Lake, P. M. Bommer, R. E. Lewis, M. J. Weber, and J. M. Calderin, 'Rheological and yield stress measurements of non-Newtonian fluids using a Marsh Funnel', *J. Pet. Sci. Eng.*, vol. 77, no. 3–4, pp. 393–402, Jun. 2011.
[36] A. D. A. Givanildo, 'Mise au point de procédures d'essais mécaniques sur mortiers de terre, application à l'étude de leur rhéologie', 2005.
[37] J.-C. Baudez, F. Chabot, and P. Coussot, 'Rheological Interpretation of the Slump Test', *Appl. Rheol.*, vol. 12, no. 3, pp. 133–141, Jun. 2002.
[38] G. Alhaik *et al.*, 'Enhance the rheological and mechanical properties of clayey materials by adding starches', *Constr. Build. Mater.*, vol. 139, pp. 602–610, May 2017.
[39] D18 Committee, 'Test Method for Marsh Funnel Viscosity of Clay Construction Slurries', ASTM International.
[40] AFNOR, 'SNF EN ISO 2431'. .
[41] M. Sonebi, L. Svermova, and P. J. M. Bartos, 'Statistical modelling of cement slurries for self-compacting SIFCON containing silica fume', p. 9, 2003.
[42] *NF P 94-054 Soils : investigation and testing - Determination of particle density - Pycnometer method*. 1991.
[43] F. Mahaut, S. Mokéddem, X. Chateau, N. Roussel, and G. Ovarlez, 'Effect of coarse particle volume fraction on the yield stress and thixotropy of cementitious materials', *Cem. Concr. Res.*, vol. 38, no. 11, pp. 1276–1285, Nov. 2008.
[44] A. Perrot, T. Lecompte, P. Estellé, and S. Amziane, 'Structural build-up of rigid fiber reinforced cement-based materials', *Mater. Struct.*, vol. 46, no. 9, pp. 1561–1568, Sep. 2013.
[45] C09 Committee, 'Test Method for Slump of Hydraulic-Cement Concrete', ASTM International.
[46] C01 Committee, 'Specification for Flow Table for Use in Tests of Hydraulic Cement', ASTM International.

[47] A. Pierre, C. Lanos, and P. Estellé, ‘Extension of spread-slump formulae for yield stress evaluation’, p. 23, 2013.
[48] N. Roussel and P. Coussot, ‘“Fifty-cent rheometer” for yield stress measurements: From slump to spreading flow’, *J. Rheol.*, vol. 49, no. 3, pp. 705–718, May 2005.
[49] J. Engmann, C. Servais, and A. S. Burbidge, ‘Squeeze flow theory and applications to rheometry: A review’, *J. Non-Newton. Fluid Mech.*, vol. 132, no. 1–3, pp. 1–27, Dec. 2005.
[50] G. Lombardi, ‘The role of cohesion in cement grouting of rock’, *15ème Congrès des Grands Barrages, Lausanne*, Suisse, 1985.
[51] S. Amziane, A. Perrot, and T. Lecompte, ‘A novel settling and structural build-up measurement method’, *Meas. Sci. Technol.*, vol. 19, no. 10, p. 105702, Oct. 2008.
[52] M. Maillard, J. Bleyer, A. L. Andrieux, J. Boujlel, and P. Coussot, ‘Dip-coating of yield stress fluids’, *Phys. Fluids*, vol. 28, no. 5, p. 053102, May 2016.
[53] P. Coussot, ‘Steady, laminar, flow of concentrated mud suspensions in open channel’, *J. Hydraul. Res.*, vol. 32, no. 4, pp. 535–559, Jan. 1994.
[54] A. Pierre, A. Perrot, A. Histace, S. Gharsalli, and E.-H. Kadri, ‘A study on the limitations of a vane rheometer for mineral suspensions using image processing’, *Rheol. Acta*, vol. 56, no. 4, pp. 351–367, Apr. 2017.
[55] ‘Pierre et al. - 2017 - A study on the limitations of a vane rheometer for.pdf’. .
[56] S. Clayton, T. G. Grice, and D. V. Boger, ‘Analysis of the slump test for on-site yield stress measurement of mineral suspensions’, *Int. J. Miner. Process.*, vol. 70, no. 1–4, pp. 3–21, Jun. 2003.